The Study on the Dynamics and Friction Characteristics of Piston Skirt with Consideration of Mixed Lubrication

Kim, Ji-Young*
Graduate student, Seoul National University
Han, Dong-Chul
Professor, Seoul National University
Cho, Myung-Rae, Choi Jae-Kwon
Power Train R&D Center, Hyundai Motor Co. Ltd.

This paper reports on the dynamics and friction characteristics of piston skirt with consideration of mixed lubrication. Piston skirt is an important part of the engine that transforms fuel into mechanical energy. The durability and low friction characteristics are important recent issues in piston skirt design. In this paper, the piston skirt motion is analyzed with consideration of mixed lubrication and piston skirt tilting motion. The entire trajectory of piston motion is obtained by using transient numerical method. Also various parameter studies are performed for piston skirt design and the development of lower frictional engine.

Key Words : Mixed Lubrication, Piston Skirt, Average Flow Model, Asperity Contact, Roughness

Nomenclature

A	: Bearing Surface Area
a	: Distance from the top of skirt to the pin
b	: Distance from the top of skirt to the C. G.
C	: Clearance betw. Skirt and cylinder
C_g	: Distance betw. C. G. and wrist-pin
C_p	: Distance betw. wrist-pin and piston center
E	: Young's Modulus
e_b	: Eccentricity of piston bottom
e_t	: Eccentricity of piston top
$\dot{e}_b$	: Radial velocity of piston bottom
$\dot{e}_t$	: Radial velocity of piston top
F	: Total normal force
F_c	: Asperity contact normal force
F_{con}	: Connecting rod force
F_f	: Total friction force
F_{fc}	: Asperity contact friction force
F_{fh}	: Hydrodynamic friction force
F_{gas}	: Combustion gas force
F_h	: Hydrodynamic normal force
F_{pinx}	: Inertia force due to pin mass in x-direction
F_{piny}	: Inertia force due to pin mass in y-direction
F_{pisx}	: Inertia force due to piston mass in x-direction
F_{pisy}	: Inertia force due to piston mass in y-direction
h	: Nominal film thickness
$\overline{h}$	: Non-dimensional oil film thickness
h_t	: Local oil film thickness
$\overline{h}_t$	: Average gap
I_{pis}	: Piston moment of inertia
L	: Piston-skirt length
l	: Connecting rod length
M	: Total moment about wrist-pin
M_c	: Asperity contact moment
M_f	: Total friction moment
M_{fc}	: Friction moment due to asperity contact
M_{fh}	: Friction moment due to

* Corresponding Author,
E-mail : jink@amed.snu.ac.kr
TEL : +82-2-880-8049; **FAX** : +82-2-882-3718
San 56-1, Shinlim-dong, Kwanak-ku, Seoul 151-742, Korea.(Manuscript **Received** November 21, 2000; **Revised** March 14, 2001)

hydrodynamic
M_h : Hydrodynamic moment
$M_{p:s}$: Inertia moment of piston-skirt
$m_{p:n}$: Wrist-pin mass
$m_{p:s}$: Piston-skirt mass
P_h : Hydrodynamic pressure
P_c : Asperity contact pressure
R : Nominal radius of piston-skirt
$R(\tilde{\theta}, y)$: Function of skirt surface profile
r : Crank radius
t : Time
U : Sliding speed
V_{r1}, V_{r2} : Variance ratio, $V_{r1}=\left(\frac{\sigma_1}{\sigma}\right)^2$
$\dot{Y}$, $\ddot{Y}$: Piston-skirt velocity, acceleration
α : Piston-skirt bearing angle
β : Asperity radius of curvature
δ : Composite roughness amplitude
ε_b : Dimensionless eccentricity of piston bottom
ε_t : Dimensionless eccentricity of piston top
$\dot{\varepsilon}_b$: Dimensionless velocity of piston bottom
$\dot{\varepsilon}_t$: Dimensionless velocity of piston top
ϕ_x, ϕ_y : Pressure flow factor
ϕ_s : Shear flow factor
ϕ_f, ϕ_{fp}, ϕ_{fs} : Shear stress factor
ϕ : Connecting rod angle
γ : Roughness pattern parameter
η : Oil viscosity
μ : Asperity density
μ_f : Friction coefficient
θ : Angular coordinate around piston-skirt
$\tilde{\theta}$: Bearing angular coordinate($=\theta+\alpha$)
σ : Composite rms roughness, $\sigma=\sqrt{\sigma_1^2+\sigma_2^2}$
τ : Hydrodynamic component of shear stress
ω : Rotational speed
ψ : Crank angle

1. Introduction

Because fuel economy is the most important aspect of modern engine design, it is necessary to reduce the frictional power losses in internal combustion engine. It is well known that piston assembly accounts for approximately half of the total engine friction and piston skirt contributes about 40% of the total friction of the piston assembly. The piston-skirt ideally operates in the hydrodynamic lubrication regime. However, direct contact between the skirt and the cylinder bore can be caused by secondary piston motion. The direct contact results in wear of the skirt and the bore, and increases the frictional loss. Therefore, accurate understanding of piston-skirt motion is essential for the reduction of frictional loss and the insurance of engine durability.

Much research on the theoretical prediction of piston motion has been performed. Knoll, et al. (1982) performed a hydrodynamic lubrication analysis for the piston skirt and presented the load-carrying capacity of the piston-skirt. The significant results for the piston motion was presented by Li, et al. (1983), Suzuki, et al. (1987). They analyzed the effects of arbitrary surface profile of the piston-skirt and the wrist-pin offset on the piston motion. Oh, et al. (1987) and Zafer, et al. (1994) performed numerical analysis for the piston motion by using the elasto-hydrodynamic theory. But they didnot consider the contact of piston and cylinder bore. In the recent years, Zhu, et al. (1992, 1993) and Liu, et al. (1998) developed a solid-to-solid contact model and calculated the piston motion by using numerical iterative method.

In this paper, an analytical model for the piston motion is presented with consideration of mixed lubrication theory. The analytical model uses the average flow model (1978, 1979) for calculating the mean hydrodynamic pressure and asperity contact model (1971) for determining the asperity contact force. The effects of roughness patterns, operating condition and design parameter on the piston motion are investigated.

2. Governing Equations

2.1 Modeling

The equations of motion in this paper are the

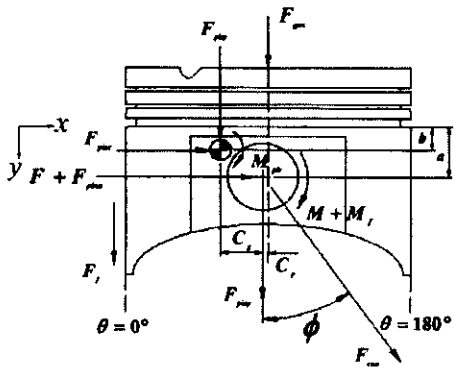

Fig. 1 Dynamic modeling of piston skirt

same but a few modifications are made as those of previous studies by Li, et al. (1983) and Zhu, et al. (1992, 1993).

A schematic diagram of the piston assembly system is shown in Fig. 1. In Fig. 1, F, F_f, M, M_f consist of hydrodynamic force and asperity contact, which are expressed as follows:

$$F=F_h+F_c,\ F_f=F_{fh}+F_{fc}$$
$$M=M_h+M_c,\ M_f=M_{fh}+M_{fc} \tag{1}$$

The combustion gas force F_{gas} is calculated by using the measured explosive gas pressure. The force equilibrium in two directions and moment equilibrium are given by the following equations:

$$F_f+F_{gas}+F_{pisy}+F_{piny}+F_{con}\cos\phi=0$$
$$F+F_{pisx}+F_{pinx}+F_{con}\sin\phi=0$$
$$M_{pis}+F_{pisx}(a-b)+M+M_f+F_{gas}C_p-F_{pisy}C_g=0 \tag{2}$$

The first and secondary motions of the piston within the given clearance between the piston-skirt and the cylinder bore are very important factors to predict the lubricant condition and for system design. The primary motion of the piston is the translation motion along the x-direction, and the secondary motion of the piston is the rotational motion about the axis of the cylinder center. From Eq. (2), the equilibrium equations for the primary and secondary motions of the piston are given by:

$$-F_{pisx}-F_{pinx}=F-(F_f+F_{gas}+F_{pisy}+F_{piny})\tan\phi$$
$$-M_{pis}-F_{pisx}(a-b)=M+M_f+F_{gas}C_p-F_{pisy}C_g \tag{3}$$

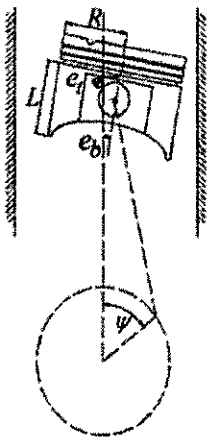

Fig. 2 Piston motion

In Eq. (3), the connecting rod angle is calculated by the following geometric analysis.

$$\phi=\arctan\left(\frac{C_p+r\sin\psi}{\sqrt{t^2-(C_p+r\sin\psi)^2}}\right) \tag{4}$$

To simplify the analysis, all forces and moments in the governing equations for the piston motion have to be expressed by piston eccentricity, velocity, and acceleration. In this paper the piston motion is described using the top and bottom eccentricities of the piston, e_t and e_b, and its velocity and acceleration (see Fig. 2).

Therefore F_{pisx}, F_{pinx}, and M_{pis} in Eq. (3) are expressed by $\ddot{e}_t$ and $\ddot{e}_b$, which are defined as follows:

$$F_{pisx}=-m_{pis}\left(\ddot{e}_t+\frac{b}{L}(\ddot{e}_b-\ddot{e}_t)\right)$$
$$F_{pinx}=-m_{pin}\left(\ddot{e}_t+\frac{a}{L}(\ddot{e}_b-\ddot{e}_t)\right)$$
$$M_{pis}=-\frac{I_{pis}(\ddot{e}_t-\ddot{e}_b)}{L} \tag{5}$$

The acceleration of piston in y-direction is determined by using the kinematics analysis, and given by:

$$\ddot{Y}=r\omega^2\cos\psi+\frac{(r\omega(C_p+r\sin\psi)\cos\psi)^2}{\sqrt{(l^2-(C_p+r\sin\psi)^2)^3}}+\frac{((r\omega\cos\psi)^2-r\omega^2(C_p+r\sin\psi)\sin\psi)}{\sqrt{(l^2-(C_p+r\sin\psi)^2)}} \tag{6}$$

Therefore, the inertia force of the piston in both directions are defined as follows:

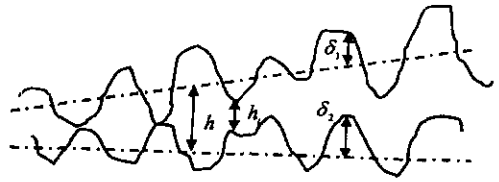

Fig. 3 Schematic diagram of surface roughness

$$F_{pisy}=-m_{pis}\ddot{Y}$$
$$F_{piny}=-m_{pin}\ddot{Y} \tag{7}$$

From the above equations, the final governing equation of the piston motion is expressed in the following matrix form:

$$\begin{bmatrix} m_{pin}\left(1-\frac{a}{L}\right)+m_{pis}\left(1-\frac{b}{L}\right) & m_{pin}\frac{a}{L}+m_{pis}\frac{b}{L} \\ \frac{I_{pis}}{L}+m_{pis}(a-b)\left(1-\frac{b}{L}\right) & m_{pis}(a-b)\frac{b}{L}-\frac{I_{pis}}{L} \end{bmatrix} \begin{Bmatrix} \ddot{e}_t \\ \ddot{e}_b \end{Bmatrix} = \begin{bmatrix} F-(F_f+F_{gas}+F_{pisy}+F_{piny})\tan\phi \\ M+M_f+F_{gas}C_p-F_{pisy}C_g \end{bmatrix} \tag{8}$$

2.2 Average reynolds equation

The Average Reynolds equation derived by Patir et al. (1978, 1979) is used in this study to consider the surface roughness effects. Two-dimensional form of the equation is written as

$$\frac{d}{dx}\left(\frac{\phi_x h^3}{\eta}\frac{dp}{dx}\right)+\frac{d}{dy}\left(\frac{\phi_y h^3}{\eta}\frac{dp}{dy}\right) = -6U\left(\frac{d\bar{h}_t}{dy}+6\sigma\frac{d\phi_s}{dy}\right)+12\frac{d\bar{h}_t}{dt} \tag{9}$$

In this study, the nominal oil film equation, considering the piston-skirt shape, is expressed as follows: (10)

$$h(\tilde{\theta}, y, t)=C+e_t\cos(\tilde{\theta}-\alpha) +(e_b-e_t)\frac{Y}{L}\cos(\tilde{\theta}-\alpha)+R(\tilde{\theta}, y) \tag{10}$$

Equations (11) and (12) define the local oil film thickness and the average gap.

$$h_t=h+\delta_1+\delta_2 \tag{11}$$
$$\bar{h}_t=\int_{-h}^{\infty}(h+\delta)f(\delta)d\delta \tag{12}$$

δ is the composite roughness and $f(\delta)$ is the probability density function of δ.

By adapting the following nondimensional variables,

$$\bar{\theta}=\frac{x}{R},\ \bar{y}=\frac{y}{R},\ H=\frac{h}{\sigma},\ \bar{h}=\frac{h}{\sigma},$$

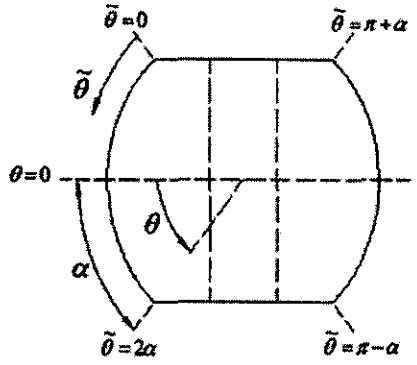

Fig. 4 Hydrodynamic and contact pressure analysis domains of two lubricated surfaces of piston skirt

$$\bar{p}=\frac{p(C/R)^2}{\eta_0\omega}$$
$$\eta^*=\frac{\eta}{\eta_0},\ \bar{U}=\frac{U}{r\omega},\ \tau=\omega t,\ \phi_c=\frac{d\bar{h}_t}{dh}$$

Equation (8) is normalized as follows

$$\frac{d}{d\bar{\theta}}\left(\frac{\phi_x\bar{h}^3}{\eta^*}\frac{d\bar{p}}{d\bar{\theta}}\right)+\frac{d}{d\bar{y}}\left(\frac{\phi_y\bar{h}^3}{\eta^*}\frac{d\bar{p}}{d\bar{y}}\right) =-6\frac{r}{R}\bar{U}\phi_c\frac{\partial\bar{h}}{\partial\bar{y}} -6\frac{r}{R}\frac{\sigma}{C}\bar{U}\frac{\partial\phi_s}{\partial\bar{y}}+12\phi_c\frac{d\bar{h}}{d\tau} \tag{13}$$

Equation (13) is solved to obtain the hydrodynamic oil film pressure using the classical Reynolds boundary condition, which is given by:

$$\bar{p}(\tilde{\theta}=0)=\bar{p}(\tilde{\theta}=2\alpha)=0$$
$$\bar{p}(\tilde{\theta}=\pi-\alpha)=\bar{p}(\tilde{\theta}=\pi+\alpha)=0 \tag{14}$$

The hydrodynamic normal force and moment are calculated by the following equations:

$$F_h=R\iint_A P_h\cos(\tilde{\theta}-\alpha)d\tilde{\theta}dy \tag{15}$$
$$M_h=R\iint_A P_h(a-y)\cos(\tilde{\theta}-\alpha)d\tilde{\theta}dy \tag{16}$$

The hydrodynamic friction force and moment are calculated by the following equations using the previous study of Patir and Cheng(1979):

$$\tau=-\frac{\mu U}{\bar{h}}(\phi_f+\phi_{fs})+\phi_{fp}\frac{\bar{h}}{2}\frac{\partial P_h}{\partial y} \tag{17}$$
$$F_{fh}=R\iint_A \tau d\theta dy \tag{18}$$
$$M_{fh}=\mu_f R\iint_A \tau(R\cos(\tilde{\theta}-\alpha)-C_p)d\tilde{\theta}dy \tag{19}$$

2.3 Asperity contact model

According to the asperity contact model of Greenwood et al. (1970), the average contact pressure and contact area are expressed as follows:

$$p_c(H)=\frac{8\sqrt{2}}{15}\pi(\mu\beta\sigma)^2E\sqrt{\frac{\sigma}{\beta}}F_{2.5}(H) \quad (20)$$

In Eq. (20), for the surface roughness with Gaussian distributed asperity height, the function $F_n(H)$ is defined as:

$$F_n(H)=\frac{1}{\sqrt{2\pi}}\int_H^\infty (s-H)^n e^{-\frac{s^2}{2}}ds \quad (21)$$

Therefore, the asperity contact force and boundary friction force are calculated by the following equations

$$F_c=R\iint_A P_c\cos(\tilde{\theta}-\alpha)d\tilde{\theta}dy \quad (22)$$

$$F_{fc}=-\mu_f\frac{\dot{Y}}{|\dot{Y}|}R\iint_A P_c\cos(\tilde{\theta}-\alpha)d\tilde{\theta}dy \quad (23)$$

In the same way, asperity contact moment (M_c) and asperity contact friction moment (M_{fc}) can be obtained by:

$$M_c=R\iint_A P_c(a-y)\cos(\tilde{\theta}-\alpha)d\tilde{\theta}dy \quad (24)$$

$$M_{fc}=\mu_f R\frac{\dot{Y}}{|\dot{Y}|}\iint_A P_c(R\cos(\tilde{\theta}-\alpha)-C_p)d\tilde{\theta}dy \quad (25)$$

3. Numerical Method

The numerical procedure for obtaining the trajectory of the piston motion is as follows:

1. The initial value of e_t, e_b, $\dot{e}_t$, and $\dot{e}_b$ is assumed.
2. The fluid film thickness and flow factors are calculated. The flow factor (ϕ_x, ϕ_y, ϕ_s), contact factor (ϕ_c), and shear stress factor (ϕ_f, ϕ_{fs}, ϕ_{fb}) can be determined by the previous study of Patir and Cheng (1979).
3. The pressure distribution is calculated by using the SOR method for solving Eq. (13), and asperity contact pressure is obtained by using Eq. (20).
4. All the applied forces and moments of the oil film and the asperity contact are obtained by using numerical integration.

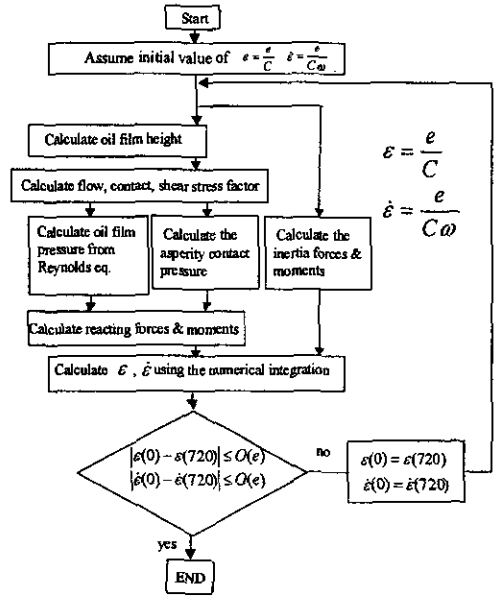

Fig. 5 Program flow chart

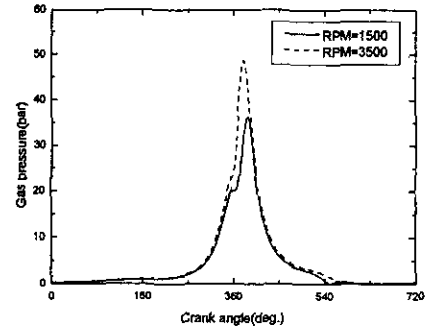

Fig. 6 Combustion gas pressure

5. The new values of and are determined by using the fourth-order Runge-Kutta method for solving Eq. (8). The procedure is repeated until convergence for the trajectory of the piston motion is achieved.

4. Result and Discussion

Figure 6 represents the measured combustion gas pressure at 1500 and 3500rpm. The peak pressure slightly increases as an engine speed up. Figure 7 shows the entire trajectory of the piston skirt motion during 4 cycles. It shows that the skirt tilts repeatedly and inclines to the left side of the cylinder bore. This is very similar to the

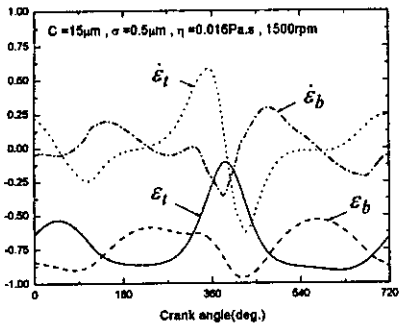

Fig. 7 The entire trajectory of piston skirt motion

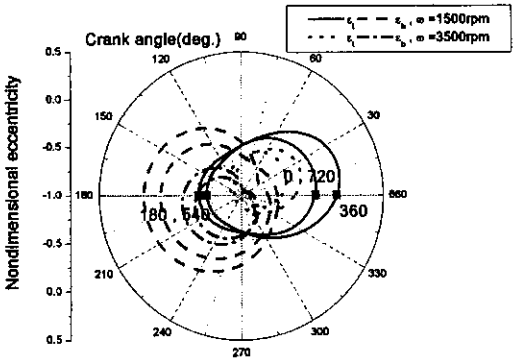

Fig. 8 The position of piston skirt top and bottom according to the operating speed

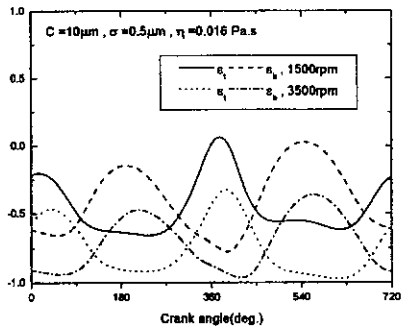

Fig. 9 Calculated results of piston motion according to the operating speed

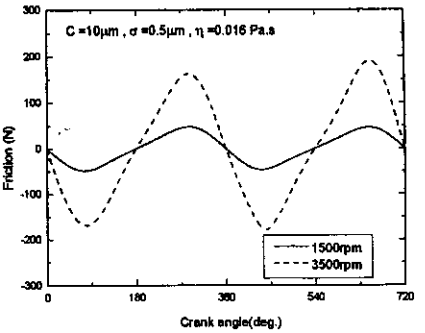

Fig. 10 Calculated results of friction force according to the operating speed

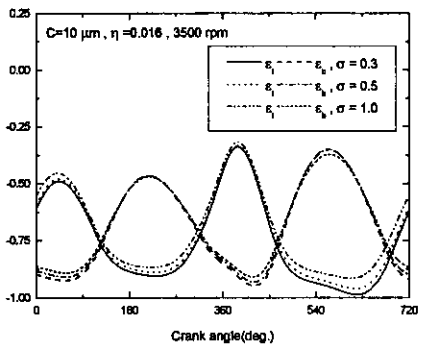

Fig. 11 Calculated results of the piston motion according to the roughness height

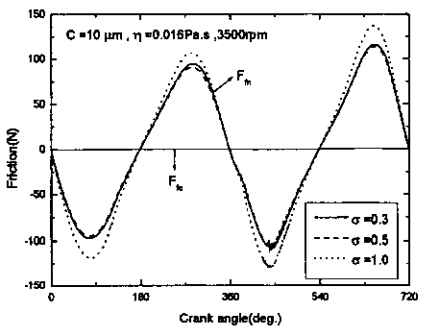

Fig. 12 Calculated results of the friction force according to the roughness height

previous result of Zhu, et al. (1992)

Figure 8 represents the oil film thickness. The center point represents the left side of the cylinder bore. In Fig. 8, as the operating speed becomes higher, the oil film thickness decreases. In other words, the center of the piston moves to the cylinder wall because of the higher slap force caused by the high engine speed. The friction force is increased because of higher shearing rate in the oil film at the high engine speed. There is no significant asperity contact during the whole engine cycle.

Figure 11 shows the results of the piston secondary motion according to the roughness rms height. An isotropic roughness pattern is considered in this paper. When the roughness

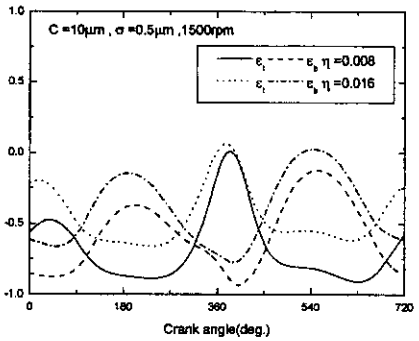

Fig. 13 Calculated results of the piston motion according to the oil viscosity

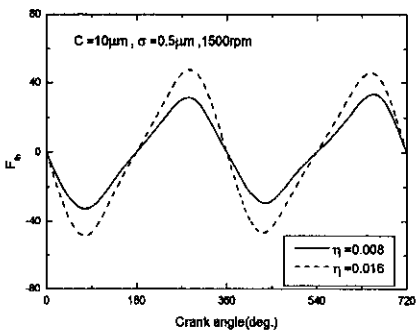

Fig. 14 Calculated results of the friction force according to the oil viscosity

height increases, the amplitude of the piston motion is reduced. The increase in roughness height results in the reduction of radial clearance. Also the increase in roughness height results in the increase in the friction force.

Figures 13 and 14 represent cases with two different viscosity coefficients. At a low viscosity, the motion of the skirt increases due to weaker hydrodynamic action in the oil film, but the friction force decreases. These results agree with hydrodynamic characteristics in the *Stribeck* diagram.

Figures 15, 16 and 17 represent cases with two different masses. For a light skirt, the oil film thickness increases and the friction force decreases. This means that the engine durability and fuel economy can be improved by reducing the piston skirt mass.

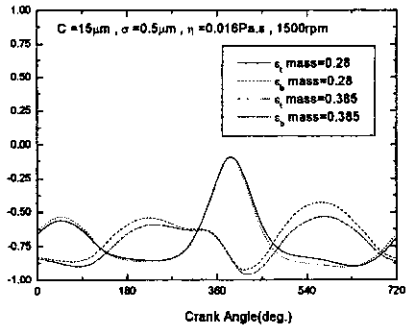

Fig. 15 Calculated results of the piston motion according to the mass

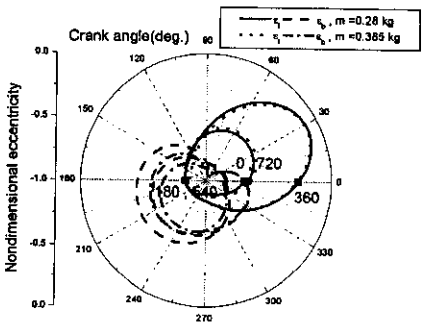

Fig. 16 The position of piston skirt top and bottom according to the mass

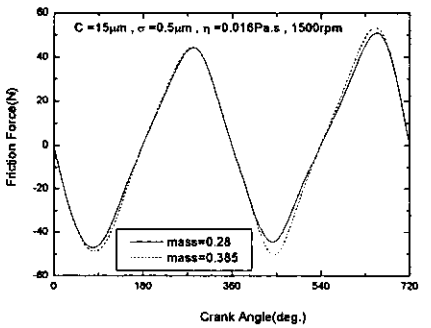

Fig. 17 Calculated results of the friction force according to the mass

5. Conclusion

This paper describes the dynamics and friction characteristics of the piston skirt with the consideration of mixed lubrication theory. The following conclusions are derived.

(1) The trajectory of the piston skirt can be

easily obtained by using the transient method.

(2) Decreasing the surface roughness, controlling the oil viscosity, and using low weight skirt can reduce the friction force and power loss in the piston skirt. For example, the total power loss can be reduced by about 5.5% by using low weight piston skirt. Besides, frictional power loss and piston skirt motion vary significantly according to the engine operating speed.

(3) It is thought that the above analytical model is a useful tool to verify and enhance the tribological performance of the designed piston skirt system.

Acknowledgement

This work was supported by the Institute of Advanced Machinery and Design at Seoul National University, Korea and in part by a grant from the BK-21 Program for Mechanical and Aerospace Engineering Research at Seoul National University.

References

Greenwood, J. A and Tripp, J. H., 1970~1971, "The Contact of Two Nominally Flat Rough Surfaces," *Proc. Inst. Mech. Eng*, Vol. 185, Part 1, No. 48, pp. 625~633.

Knoll, G.D. and Peeken, H.J, 1982, "Hydrodynamic Lubrication of Piston Skirts," *ASME Journal of Tribology*, Vol. 104, pp. 504~509.

Li, D.F., and Rohde, S. M., 1983, "An Automotive Piston Lubrication Model, ASLE Transactions," Vol. 26, pp. 151~160.

Liu, K. and Xie, Y. B., 1998, "A Comprehensive study of the friction and dynamic motion of the piston assembly," *Proc. Instn. Mech. Engrs.*, Vol. 212, pp. 221~226.

Patir, N. and Cheng, H. S., 1978, "An Average Flow Model for Determining Effects of Three-Dimensional Roughness on Partial Hydrodynamic Lubrication," *ASME Journal of Tribology*, Vol. 100, pp. 12~17.

Patir, N. and Cheng, H. S. 1979, "Trans. Application of Average Flow Model to Lubrication Between Rough Sliding Surfaces," *ASME Journal of Tribology*, Vol. 101, pp. 220~230.

Oh, K.P. and Li, C.H., 1987, "Elastohydrodynamic Lubrication of Piston Skirt," *ASME Journal of Tribology*, Vol. 109, pp. 356~362.

Suzuki, T., Fujimoto, Y., Ochiai, Y., and Fujimura, I., 1987, "A Numerical Study on Piston Slap in Diesel Engines," *JSME Transactions*, Series B, Vol. 53, No. 492, pp. 2610~2618.

Wu, C. and Zheng, L., 1989, "An Average Reynolds Equation for Partial Film Lubrication with a Contact Factor," *ASME Journal of Tribology*, Vol. 111, pp. 188~191.

Zafer,. D. et al., 1994, "A Model of Piston Secondary Motion and Elastohydrodynamic Skirt Lubrication," *ASME Journal of Tribology*, Vol. 116, pp. 777~785.

Zhu, D. and Cheng, H. S., 1992, "A Numerical Analysis for Piston Skirts in Mixed Lubrication-Part I : Basic Modeling," *ASME Journal of Tribology*, Vol. 114, pp. 553~562.

Zhu, D. and Cheng, H. S., 1993, "A Numerical Analysis for Piston Skirts in Mixed Lubrication-Part II : Deformation Considerations," *ASME Journal of Tribology*, Vol. 115, pp. 125~133.